AUTOMATED DAMAGE ASSESSMENT FROM 3-D LASER SCANS

B. Guldur[1] and J. F. Hajjar[2]

ABSTRACT

Many existing bridges suffer from damage due to age or accumulated damage from hazards. It is essential to accurately assess the current conditions of these aging, deteriorating and damaged structures in order to evaluate their present status and decide on future steps for rehabilitation. Three-dimensional laser-scanning technology, which is used to collect 3D laser scans with coupled texture-mapped images, is a common way to capture the as-is conditions of structures. However, it is challenging to automatically extract meaningful information from the high-resolution laser scans even though they provide a detailed geometric representation. Dividing the collected 3D laser scan into useful clusters requires determining the location, orientation and size of objects in a scene by using well-established point cloud processing steps. Once the objects are detected, they are used for identifying the deteriorated locations. This paper describes several new methods developed for automatically locating, quantifying and documenting damage types including large cracks, spalling and misalignment from 3D laser scans. Proposed methods are tested on a collapsed bridge scan, in order to show that defect localization and quantification are performed successfully. The obtained results show that 3D laser-scanning technology could be effectively used to document critical, quantitative information on present conditions related to damage of structures.

[1]Graduate Research Assistant, Dept. of Civil and Env. Eng., Northeastern University, Boston, MA 02115
[2]Professor and Chair, Dept. of Civil and Env. Eng., Northeastern University, Boston, MA 02115

Guldur B., Hajjar J.F. Automated Damage Assessment from 3-D Laser Scans. *Proceedings of the Istanbul Bridge Conference*, 2014.

Automated Damage Assessment from 3-D Laser Scans

B. Guldur[1] and J. F. Hajjar[2]

ABSTRACT

Many existing bridges suffer from damage due to age or accumulated damage from hazards. It is essential to accurately assess the current conditions of these aging, deteriorating and damaged structures in order to evaluate their present status and decide on future steps for rehabilitation. Three-dimensional laser-scanning technology, which is used to collect 3D laser scans with coupled texture-mapped images, is a common way to capture the as-is conditions of structures. However, it is challenging to automatically extract meaningful information from the high-resolution laser scans even though they provide a detailed geometric representation. Dividing the collected 3D laser scan into useful clusters requires determining the location, orientation and size of objects in a scene by using well-established point cloud processing steps. Once the objects are detected, they are used for identifying the deteriorated locations. This paper describes several new methods developed for automatically locating, quantifying and documenting damage types including large cracks, spalling and misalignment from 3D laser scans. Proposed methods are tested on a collapsed bridge scan, in order to show that defect localization and quantification are performed successfully. The obtained results show that 3D laser-scanning technology could be effectively used to document critical, quantitative information on present conditions related to damage of structures.

Introduction

The most recent ASCE Report Card for America's infrastructure, which depicts the condition and performance of the nation's infrastructure, was released in 2013 [1]. In this report, the average grade for all infrastructure types was a D+. This demonstrates the importance of assessing the current condition of our infrastructure by performing recurring inspections and taking necessary precautions based on these up-to-date assessment results.

Currently, inspections are generally conducted by using the data collected from discrete sensor locations and/or visual inspections that are carried out by trained experts. Both of these inspection methods have challenges. First, even if the sensors mounted on structures record accurate data for any measured quantity, they do not represent the complete surface behavior of the investigated structure since they are discretely located. Second, visual inspections often involve shutting down a portion of the structure and sending out trained experts for executing the inspections. This method is dangerous, time consuming, expensive, and subjective, since the results of each inspection depend on the personal judgment of the inspector. On the other hand, laser scanning technology is an accurate and contactless inspection option that provides continuous surface data even for hard to reach locations. Collected datasets may be updated, and they enable the repeatable evaluation of structures.

[1]Graduate Research Assistant, Dept. of Civil and Env. Eng., Northeastern University, Boston, MA 02115
[2]Professor and Chair, Dept. of Civil and Env. Eng., Northeastern University, Boston, MA 02115

Guldur B., Hajjar J.F. Automated Damage Assessment from 3-D Laser Scans. *Proceedings of the Istanbul Bridge Conference*, 2014.

This paper highlights two new surface damage detection methods on a portion of the point cloud collected from a collapsed bridge located near Dekalb County, Illinois. The details of each surface damage method are described below.

DeKalb County Bridge

The point cloud shown in Figure 1 was collected from a collapsed bridge near DeKalb County, Illinois. This bridge was located in a rural area and consisted of a precast concrete deck, reinforced concrete pier caps, and timber piers. One set of timber piers failed, causing the bridge deck to collapse at that location. The forensic investigation of the collapse is available in Borello et al. [2].

Fourteen scans of the scene were captured from different locations around the structure with a Faro Photon 80 scanner, which has a range of accuracy within ±2 mm. Figure 1 shows the point cloud of the entire collapsed bridge and the processed portion of it.

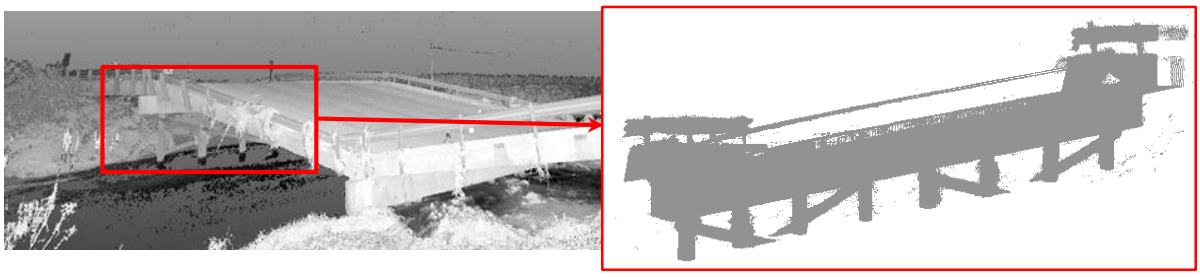

Figure 1: Point cloud of the entire DeKalb County Bridge and the processed portion of the dataset.

Point Cloud Processing

Individual objects that form structures cannot be differentiated from raw point clouds. In order to extract element information from point clouds, it is necessary to perform point cloud processing. Point cloud processing is a general term for the steps that are required for reducing complexity of 3D datasets and separate elements and/or surfaces in terms of clusters.

The main steps of point cloud processing can be listed as registration, neighborhood size selection, outlier point removal, surface normal estimation, curvature estimation, extraneous point removal, feature detection, region growing for segmentation, and object detection. More information on point cloud processing can be found in Rusu et al. [3], Vosselman [4] and Walsh et al. [5]. Even though the details of the listed point cloud processing steps are not discussed in this paper, it is important to understand the basic principles of each step since the developed surface damage detection algorithms are directly related to them.

Laser-based Surface Damage Detection

In this paper, two surface damage detection strategies, which can be listed as graph-based surface damage detection and surface normal-based surface damage detection, are discussed. The application of these methods on the collapsed bridge dataset shown in Figure 1 is represented in the following sections of this paper.

The surface damage detection methods are specifically developed for segmented point cloud datasets. The segmented point clouds, also referred to as clusters, are obtained after performing the point cloud processing steps discussed above, starting with registration and ending with object detection. Thus, the individual datasets used in this paper are already established as clusters.

Preprocessing Steps for Surface Damage Detection

Point clouds that are collected via laser scanners generally have a significant amount of noise along with extraneous points that do not belong to the underlying surface. Extraneous points can either be a part of an object that is attached to main surfaces or they can belong to an object that occludes them. Noise and extraneous points need to be removed from the point cloud clusters before applying the proposed surface damage detection algorithms.

In this research, to remove noise from point clouds, a statistical outlier removal method is applied [6]. This method uses the number of neighborhood points k which is calculated by using the 'k nearest neighborhood' method described in Hoppe et al. [7]. k is used to compute the distance distribution of each point from its neighborhood points in the investigated cluster. This distribution is assumed to be Gaussian. The noise removal criterion is defined by the mean of the calculated distances μ_d and the standard deviation $n \cdot \sigma_d$ where n represents the standard deviation multiplier. Points violating the defined criteria are removed from the point cloud. For this research, $k = 16$ and n = 1 are used as the parameters of the statistical outlier removal.

Extraneous points are removed by using a curvature criterion. First, surface curvature γ of each point of a cluster is calculated by using the method given in Pauly et al. [8]. Later, the mean value of computed variations μ_γ, and their standard deviation σ_γ, are calculated for the remaining point cloud after statistical outlier removal. A criterion similar to the statistical outlier removal method is adapted. In this study, $k = 16$ and n = 2 are used for the extraneous point removal. Since computed surface curvatures are very sensitive to local surface variations, the n value is increased to 2 in order to overcome excessive point removal.

Graph-based Surface Damage Detection

The first method used for surface damage detection is called graph-based surface damage detection. This method uses skeletons of a detected object for localizing and quantifying local defects. This is a new approach for detecting defects due to local discrepancies through point cloud processing by using object detection and model comparison [9].

First, the voxel model of the unorganized point cloud cluster is extracted and this model is used to create a 3D binary image. Second, this 3D binary image is divided into 2D binary images along the length of a cluster (cross-section cuts); subsequently, these images are processed by thinning and/or distance transformation to produce skeleton-graphs and also used to calculate both 2D and 3D shape descriptors.

Voxelization

The voxelization method used in this paper is a point-based voxelization technique, which allows direct point cloud processing since it does not require an initial surface model of the investigated object.

Details of the adapted voxelization method are given in Hinks [10]. This method consists of three main steps: construction of a voxel grid based on the laser point clouds, mapping of the given laser point cloud to the generated voxel grid, and determination of active voxels based on the performed point mapping. Active voxels are determined based on point mapping results once a suitable voxel grid is created. The voxel grid is a volumetric representation of an investigated cluster and it can be reduced to 2D binary images by assigning an appropriate height function. In this paper, a constant voxel size of 0.1 inches is used for all axes, x, y and z. This grid size is determined from the average point density of the entire point cloud.

Skeletonization

Voxelization is followed by skeletonization, which extracts information on topology. Topology is an important shape characteristic for both 2D and 3D models. First, skeletal-graph based techniques are used to compute the skeleton of the investigated cluster. Later, the shape descriptors of the model are obtained by converting this skeleton into a skeletal graph [11].

In this study, only the 3D skeleton properties are used since the objects that are present in the dataset shown in Figure 1 do not require 2D skeletonization for damage localization and quantification. Thus, only the height function with ½ inch increments is used to create the necessary skeletons. The skeleton is later used to determine alignment of the objects in the scene. The alignments of the timber piers are calculated accordingly as an example.

Defect Localization and Quantification

Defects such as material loss, element discontinuity or deformed locations are located and quantified by comparing as-is conditions of the structure with the detected object model. Cross-sectional cuts of sections are used to calculate the area of the section along the length of the member for each point cloud cluster, and the results are compared with the model perimeter at the same location by using an iterative closest point algorithm [12]. The method for calculating the areas of the damaged regions is discussed in 'Surface Normal-based Surface Damage Detection'. The change in the volume of an object is calculated by integrating the areas of the cross-sectional cuts along the skeleton. Figure 2 represents example skeletons for bent and discontinuous members and the cross-sectional cuts of modal and as-is condition of a damaged C-section.

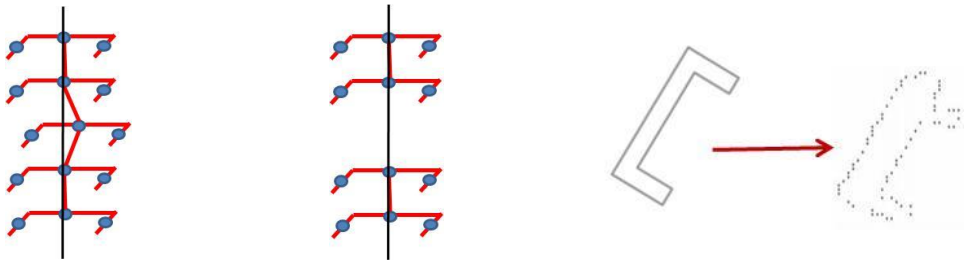

(a) Bent Members Discontinuities (c) Rupture/Spalling

Figure 2. (a) Skeleton of a bent member, (b) skeleton of a discontinuous member and (c) modal and point cloud section cut of a C-section.

Surface normal-based Surface Damage Detection

The surface normal-based surface damage detection relies on modal properties of detected surfaces and/or objects. The relative orientation of the estimated surface normal with respect to a reference normal is used to locate defective areas on the surface of structures. The reference normal can be a surface normal computed via surface patches, the normal representing the skeleton of the detected object, or the normal vector between a reference point and the current query point. This method is developed by adapting the crack detection method for 3D images discussed in Torok et al. [13] for point clouds with or without color information. The point cloud used in this study does not have color information.

Surface Normal Estimation

The local feature representation of a query point p_q can be estimated by using neighborhood points P_k, once the neighborhood size k is determined. Surface normal estimation is essential because it captures the local properties of every query point p_q in a given point cloud P, and the obtained local feature representation can be used to capture the geometry of the underlying sampled surface around the investigated p_q.

For this research a first order 3D plane fitting method based on Berkmann and Caelli [14] is implemented for computing the surface normal associated with each p_q. A least-square plane fitting estimation in P_k, which was described in Shakarji [15], is used to determine the normal to a point on the surface by estimating the normal of a plane tangent to the surface. Thus, the solution for estimating the surface normal $\vec{n}$ is reduced to an analysis of the eigenvectors and eigenvalues of a covariance matrix created from the nearest neighbors of the p_q. In this study, $k = 16$ is used for the surface normal estimation.

Surface Patch Investigation

Surface patch investigation is a crucial step in the pre-processing phase of the surface normal-based surface damage detection if the object information that reserves properties such as the skeleton or the reference point is not available. In this case, it is required to extract the normal orientation from the undamaged portion of the underlying surface. This normal will be compared with the surface normal associated with each query point p_q on a segmented surface. The representation of the explained situation is given in Figure 3 where the reference normal is shown with dashed arrows.

Three patches are selected from the undamaged locations automatically. This is ensured by using the curvature information. First, the point with the lowest curvature for a neighborhood size of 128 is selected as the seed point. $k = 128$ instead of $k = 16$ is used in order to capture the local changes in a larger area. Once all the neighborhood points that belong to the first patch are removed from the dataset, the second point with the lowest curvature is selected from the remaining dataset. Finally, the same steps are repeated to select the third patch for reference normal estimation. The average value of the normal estimated for these three patches is assigned as the reference normal for the surface under investigation.

Normal Comparison for Plain Point Clouds

Plain point clouds, such as the one used in this study, store only the geographic locations of

the surface points. The unavailability of the color information prevents this type of dataset to be used for detecting defects such as small cracks or corrosion. Small cracks and corrosion result in slight local changes which in most cases smoothed out during the surface normal estimation; thus, these damage types are commonly not detectable without color information.

Figure 3 represents the examples for surface damage and the normals on the damaged area $\vec{n}_i$ for the three possible schemes: in the first scheme, only the surface patches are available for reference normal $\vec{n}_r$ estimation; in the second scheme, the normal representing the skeleton of the detected object is used as the $\vec{n}_r$; and in the final scheme, the $\vec{n}_r$ is defined as the normal vector between a reference point p_r and the current query point p_q. In Figure 3, the reference normals are shown with dashed lines.

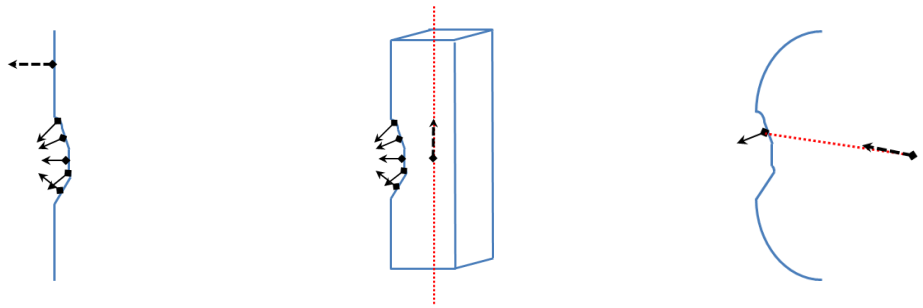

(a) (b) (c)

Figure 3. The representations of the reference normal and the normals from defect area: (a) from surface data, (b) from object with a skeleton and (c) from a surface with a reference point.

The angle α_{ri} between the $\vec{n}_r$ and each $\vec{n}_i$ is calculated. Once the α_{ri} is computed for all the points in the cluster, the computed angle values are compared with a threshold value. This angle threshold T_α is used to differentiate undamaged locations on the surface from the damaged. For this work, $T_\alpha = 10°$ is used. The points with $10° < \vec{n}_i < 170°$ are labeled as defective. Since it is not possible to determine the direction of a normal unless the viewpoint of the sensor is known; the reciprocal angle threshold (170°) is always checked.

Convex Hull for Damage Quantification

The defect locations are extracted by using the surface normal-based surface damage detection method described above. However, these algorithms do not provide quantitative results for the detected region. On the other hand, quantitative results are necessary for both documentation purposes and for determining the condition rating. Once the area and the volume of the defective region is calculated, this information is used to find the condition rating based on the criteria given in 'Condition Assessment based on Laser-based Damage Detection'.

The labeled points at each defect location are defined as P_{di}. The convex hull of P_{di}, which is either in the Euclidian plane (area) or the Euclidian space (volume), is the smallest convex set that contains P_{di}. The convex hull can be visualized as a band (area) or surface (volume) stretched around P_{di}. The computed convex set produces a closed perimeter in 2D or a watertight volume in 3D. The perimeter is used to calculate the current area of the cross-section, and the watertight volume is directly used for estimating the volume lost.

P_{di} is in 3D unless the defect is a small crack or corrosion. Since the scope of this work excludes small cracks and corrosion, it can be assumed that all of the P_{di} point sets will be in 3D space. In this case, the convex hull approach can be directly applied to compute the volume. However, an intermediate step is needed to calculate the area for each damaged location. For the defects that occur on a planar surface, the area is calculated by using the area obtained by projecting the points on to the surface where the reference normal is computed. For any other surface type, a plane is fitted to the P_{di} by using the least-squares approach and the average error is computed. Error is defined as the closest distance from each point to a fitted plane. The average error is used as the height of the defect and an average value for the area is calculated by dividing the volume by the average error value.

Condition Assessment based on Laser-based Damage Detection

The final step of the surface damage detection is to determine the condition rating of the structural items. This is obtained by comparing the current physical state of the structure to what it was the day it was built. This process is important since the visual inspection based condition rating is the first part of the structural evaluation, which gives the overall condition of the structure based on all major deficiencies and its ability to carry loads. The aim is to classify the damage severity and to assign labels to the detected damage in a well-known format based on sample condition rating guidelines.

The point cloud used for this study consists of a concrete deck and timber piers. Thus, only the condition rating criteria for these two types of items is considered. The Ohio Department of Transportation has a very detailed condition rating outlines for several items on bridges. The guidelines given in the Manual of Bridge Inspection of the Ohio Department of Transportation [16] are used to get the concrete deck rating. However, this manual does not include rating guidelines for substructural items composed of timber. In order to rate the timber piers, the National Bridge Inventory Condition Ratings listed by the Federal Highway Administration [17] is used. Table 1 lists the condition rating criteria used for both the concrete deck and the timber piers.

Results

Table 2 lists all the methods used for detecting surface damage for the processed dataset. The parameters associated with each method and the corresponding values used for this study are also included in
Table 2.

Table 3 summarizes the results of the surface damage detection algorithms for individual items of the processed point cloud of the bridge of Figure 1. The alignments of the piers are also included in
Table 3 even though Table 1 does not provide any guidelines for rating the piers based on alignment. The values listed for the alignments are not used for condition rating determination.

Conclusions

This paper presents two methodologies for detecting the existing surface damage on bridges

by using laser scanning technology. The graph-based surface damage detection method uses object information for locating and quantifying the existing surface damage on structures whereas the surface normal-based damage detection method uses local variations on the surfaces of investigated structures for defect detection purposes. Both methods provide

Table 1. Condition rating criteria for concrete deck and substructure that contains timber piers.

Rating			Concrete Deck			Substructure
			Spalling with Exposed Reinforcement	Damp or Dark Areas or Saturation	Cracks	Timber
			% of area not including the fascias			
1	9	Excellent	No signs of distress, no discoloration.			No noticable or noteworthy deficiencies which affect the condition of the substructure item.
	8	Very Good	Minor delaminations, minor spalling.	Minor discoloration.	Isolated hairline cracking with no rust staining, no dampness, no leakage.	Insignificant damage caused by drift or collision with no misalignment and no corrective action required.
	7	Good	Up to 1%	Up to 5%	Minor problems, hairline cracking with isolated leaking, efflorescence. No rust staining. Map cracking combined with mottled areas up to 5%.	Insignificant decay, cracking or splitting of timber substructure unit.
2	6	Satisfactory	Up to 5% (unsound areas up to 10%)	Up to 10%	Minor structural cracking with leaking, efflorescence and rust staining. Map cracking combined with mottled areas up to 10%.	Some initial decay, cracking or splitting of timber in a timber substructure unit. Fire damage limited to surface scorching of timber with no measurable section loss.
	5	Fair	Up to 10%, (unsound areas up to 20%) slab with more than 1/3 primary bars exposed in one transverse plane.	Up to 20%	Structural cracking with leaking, efflorescence and rust staining. Map cracking combined with mottled areas up to 20%.	Moderate decay, cracking or splitting of timber with minor, measurable section loss. Some exposure of timber piles as a result of erosion, reducing the embedment.
3	4	Poor	Combined total not exceeding 30% with more than 4 adjacent exposed reinforcing bars having greater than 10% section loss to the original diameter.		Advanced cracking with heavy leaking, efflorescence and rust staining. Hairline map cracking combined with mottled areas up to 30%.	Substantial decay, cracking, splitting or crushing of primary timber members, requiring some replacement. Fire damage with significant section loss of timber which may reduce the load carrying capacity of the member. Extensive exposure of timber piles as a result of erosion, reducing the penetration and affecting the stability of the unit.
	3	Serious	Up to 30% spalling, delamination with more than 5 adjacent reinforcing bars have greater than 25% section loss to the original diameter or up to 50% damp/dark areas			Severe section loss in critical areas. Major fire damage to timber which will substantially reduce the load carrying capacity of the member. Bearing areas seriously deteriorated with considerable loss of bearing.
4	2	Critical	More than 30% spalling, delamination with more than 10 adjacent reinforcing bars having greater than 25% section loss to the original diameter or more than 50% damp/dark areas; Evidence that full depth hole(s), leading to structural failure of the slab in the traveled lane.			Primary timber members crushed or split and ineffective. Pier has settled.
	1	Imminent Failure	Major deterioration in critical structural components or obvious vertical or horizontal movement affecting structure stability. Bridge is closed to traffic but correction action may put back in light service.			Bridge closed. Corrective action may be put back in light service.
	0	Failed	Bridge closed, collapsed.			Bridge closed. Replacement necessary.

contactless and area-wide surface inspection options for bridges. Integrating new technologies for inspections is important since there is an increasing demand for inspecting aging and deteriorating structures. Results show that laser scanners can be efficiently used for inspecting structures without having user interaction and also for documenting the outcome in a selected format. Since the results are solely dependent on the used parameters and completely repeatable, the variations on the results due to personal judgment are eliminated as well.

In future work, this research will be extended to show results on texture-mapped point clouds. Texture-mapped point clouds provide larger set of detectable defect types since small cracks and corrosion are added to the list. Determining the sensitivity of the proposed methods to the listed parameters is also important. It is required to analyze the effect of the parameter alteration on the obtained damage detection results.

Table 2. Parameters and the corresponding values for the methods used for surface damage detection.

	Methods	Parameters	Value
Preprocessing Steps	**Statistical Outlier Removal**	Neighborhood size, k	16
		Standard deviation multiplier, n	1
	Extraneous Point Removal	Neighborhood size, k	16
		Standard deviation multiplier, n	2
Graph-based Surface Damage Detection	**Voxelization**	Voxel size	0.1 in
	Skeletonization	Height function increment	0.5 in
Surface Normal-based Surface Damage Detection	**Surface Normal Estimation**	Neighborhood size, k	16
	Surface Patch Investigation	Neighborhood size, k	128
	Normal Comparison for Plain Point Clouds	Angle threshold, T_α	10°

Table 3. The results of the surface damage detection algorithms for individual items.

	Damage Area (in^2)	Damage Volume (in^3)	Alignment (in/1 ft)	Condition Rating
Deck	947.52	1326.53	-	0 - Failure
Pier cap	1.41	0.28	1.35	6 - Satisfactory
Pier 1	4.96	1.95	1.38	3 - Serious
Pier 2	4.65	1.83	1.38	3 - Serious
Pier 3	7.75	3.05	1.41	1 – Im. Failure
Pier 4	31.00	61.02	1.34	0 - Failure
Pier 5	3.72	0.73	1.41	4 - Poor
Pier 6	1.86	0.37	1.33	4 - Poor
Pier 7	3.10	1.22	1.36	3 - Serious
Pier 8	0.31	0.02	1.38	5 – Fair

Acknowledgments

This material is based upon the work supported by the National Science Foundation under Grant No. IIS-1328816 and by Northeastern University. Any opinions, findings, and conclusions expressed in this material are those of the authors and do not necessarily reflect the views of the National Science Foundation or other sponsors.

References

1. American Society of Civil Engineers. *2013 Report Card for America's Infrastructure*, 2013.
2. Borello, D.J., et al. Experimental and Analytical Investigation of Bridge Timber Piles Under Eccentric Loads. *Engineering Structures*, 2010. **32**(8): 2237-2246.
3. Rusu, R.B., et al. Towards 3D Point Cloud-based Object Maps for Household Environments. *Robotics and Autonomous Systems*, 2008. **56**(11): 927-941.
4. Vosselman, G. Advanced Point Cloud Processing. *Photogrammetric Week*, 2009. **9**: 137-146.
5. Walsh, S.B., Borello, D.J., Guldur, B., and Hajjar, J.F. Data Processing of Point Clouds for Object Detection for Structural Engineering Applications. *Computer-Aided Civil and Infrastructure Engineering*, 2013. **28**(7): 495-508.
6. Rusu, R.B., *Semantic 3D Object Maps for Everyday Manipulation in Human Living Environments*. Ph.D. Dissertation, Institute for Informatics, Technical University of Munich. Munich, Germany, 2009. pp. 284.
7. Hoppe, H., et al. Surface Reconstruction from Unorganized Points. *Proceedings of the 19th Annual Conference on Computer Graphics and Interactive Techniques*, 1992. New York City, NY.
8. Pauly, M., Gross, M., and Kobbelt, L.P. Efficient Simplification of Point-Sampled Surfaces. *IEEE Visualization, VIS*, 2002. Boston, MA.
9. Guldur, B. and Hajjar, J.F. Laser-based Automatic Cross-Sectional Change Detection for Steel Frames. *Proceedings of the 9th International Workshop on Structural Health Monitoring 2013*, 2013. Stanford University, Stanford, California.
10. Hinks, T., *Geometric Processing Techniques for Urban Aerial Laser Scan Data*. Ph.D. Dissertation, College of Engineering, Mathematical and Physical Sciences, University College Dublin. Dublin, Ireland, 2011.
11. Iyer, N., et al. Three-dimensional Shape Searching: State-of-the-art Review and Future Trends. *Computer-Aided Design*, 2005. **37**(5): 509-530.
12. Yang, C. and Medioni, G. Object Modelling by Registration of Multiple Range Images. *Image and Vision Computing*, 1992. **10**(3): 145-155.
13. Torok, M., Fard, M., and Kochersberger, K. Post-disaster Robotic Building Assessment: Automated 3D Crack Detection from Image-based Reconstructions. *Computing in Civil Engineering*, 2012: 397-404.
14. Berkmann, J. and Caelli, T. Computation of Surface Geometry and Segmentation Using Covariance Techniques. *IEEE Transactions on Pattern Analysis and Machine Intelligence*, 1994. **16**(11): 1114-1116.
15. Shakarji, C.M. Least-squares Fitting Algorithms of the NIST Algorithm Testing System. *Journal of Reseach-National Institute of Standards and Technology*, 1998. **103**: 633-641.
16. Ohio Department of Transportation. *Manual of Bridge Inspection*, 2010. pp. 397.
17. Federal Highway Administration. *National Bridge Inventory Condition Ratings*, 2008. pp. 10.